AD-A162 535 OBSTACLES AS PROBES OF THE BLAST WAVE INTERIOR IN THE NRL LASER/HANE SIMULATION EXPERIMENT(U) NAVAL RESEARCH LAB WASHINGTON DC J L GIULIANI 06 DEC 85 NRL-MR-5671 1/1

UNCLASSIFIED F/G 19/4 NL

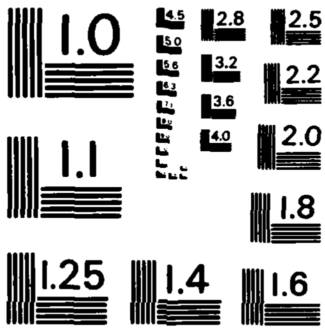

MICROCOPY RESOLUTION TEST CHART
NATIONAL BUREAU OF STANDARDS-1963-A

(2)

NRL Memorandum Report 5671

Obstacles as Probes of the Blast Wave Interior in the NRL LASER/HANE Simulation Experiment

J. L. GIULIANI, JR.

Geophysical and Plasma Dynamics Branch
Plasma Physics Division

December 6, 1985

This research was sponsored by the Defense Nuclear Agency under Subtask QIEQMXBB, work unit 00005 and work unit title "Plasma Structure Evolution."

NAVAL RESEARCH LABORATORY
Washington, D.C.

SECURITY CLASSIFICATION OF THIS PAGE

AD-A162535

REPORT DOCUMENTATION PAGE

1a REPORT SECURITY CLASSIFICATION UNCLASSIFIED	1b RESTRICTIVE MARKINGS
2a SECURITY CLASSIFICATION AUTHORITY	3 DISTRIBUTION/AVAILABILITY OF REPORT Approved for public release; distribution unlimited.
2b DECLASSIFICATION DOWNGRADING SCHEDULE	
4 PERFORMING ORGANIZATION REPORT NUMBER(S) NRL Memorandum Report 5671	5 MONITORING ORGANIZATION REPORT NUMBER(S)
6a. NAME OF PERFORMING ORGANIZATION Naval Research Laboratory 6b OFFICE SYMBOL (If applicable) Code 4780	7a NAME OF MONITORING ORGANIZATION
6c. ADDRESS (City, State, and ZIP Code) Washington, DC 20375-5000	7b. ADDRESS (City, State, and ZIP Code)
8a. NAME OF FUNDING/SPONSORING ORGANIZATION Defense Nuclear Agency 8b. OFFICE SYMBOL (If applicable) RAAE	9. PROCUREMENT INSTRUMENT IDENTIFICATION NUMBER
8c. ADDRESS (City, State, and ZIP Code) Washington, DC 20305	10 SOURCE OF FUNDING NUMBERS PROGRAM ELEMENT NO. 62715H PROJECT NO. TASK NO. WORK UNIT ACCESSION NO. DN580-072

11 TITLE (Include Security Classification)
Obstacles as Probes of the Blast Wave Interior in the NRL LASER/HANE Simulation Experiment

12 PERSONAL AUTHOR(S)
Giuliani, J.L., Jr.

13a. TYPE OF REPORT	13b. TIME COVERED	14. DATE OF REPORT (Year, Month, Day)	15. PAGE COUNT
Interim	FROM ______ TO ______	1985 December 6	37

16 SUPPLEMENTARY NOTATION This research was sponsored by the Defense Nuclear Agency under Subtask QIEQMXBB, work unit 00005 and work unit title "Plasma Structure Evolution."

17 COSATI CODES			18. SUBJECT TERMS (Continue on reverse if necessary and identify by block number)
FIELD	GROUP	SUB-GROUP	Laser/target interaction; Blast wave; Experimental diagnostics

19 ABSTRACT (Continue on reverse if necessary and identify by block number)

It is proposed that small obstacles be placed in the path of the expanding blast wave to probe the dynamics of the interior cavity formed after a laser/target interaction. The theory of attached and detached shocks for cones and spheres in supersonic streams is briefly reviewed. Graphs of the results for a ratio of specific heat $\gamma = 1.2$ and 5/3 are presented for estimating the local Mach number in the cavity from the experimental results. It is also suggested that theoretical and numerical models of the experiment predict the temporal evolution of the bow shock stand off distance for a blunt obstacle. A direct comparison with the experiment can then verify or rule out the competing models.

20 DISTRIBUTION/AVAILABILITY OF ABSTRACT ☒ UNCLASSIFIED/UNLIMITED ☐ SAME AS RPT ☐ DTIC USERS	21 ABSTRACT SECURITY CLASSIFICATION UNCLASSIFIED
22a NAME OF RESPONSIBLE INDIVIDUAL J. D. Huba	22b TELEPHONE (Include Area Code) (202) 767-3630 22c. OFFICE SYMBOL Code 4780

DD FORM 1473, 84 MAR — 83 APR edition may be used until exhausted. All other editions are obsolete

SECURITY CLASSIFICATION OF THIS PAGE

CONTENTS

OBSTACLES AS PROBES OF THE BLAST WAVE INTERIOR IN THE NRL LASER/HANE SIMULATION EXPERIMENT

I. Introduction

Over the past several years the Plasma Physics Division at the Naval Research Laboratory has developed an experimental apparatus which can simulate certain physical processes characteristic of a high altitude nuclear event (HANE).[1] This program is under the auspices of the Division of Atmospheric Effects of the Defense Nuclear Agency. It has the primary goal of a physical understanding and reliable prediction of the degradation of radar and communication systems through a HANE-disturbed atmosphere.

The first series of experiments (prior to January 1985) were initiated by irradiating a thin target with a single neodymiun laser beam. Dark-field shadowgraphy for the case of a high pressure ($\gtrsim$ 1 Torr)) ambient gas showed that the rapid heating and evaporation of the target material was followed by an expanding shock wave.[2,3]. Thus in a real HANE, as well as in the experiment, the disturbed region was bounded on the exterior by a strong shock front. However, the velocity and temperature within the disturbed region of the experimentally produced explosion has not been discerned. We will refer to this interior region as the cavity because the electron density has been found to be much lower in the interior than at the shock front.[4] Clearly the degree to which the experiment can simulate a HANE and the applicability of the laboratory results for predicting nuclear environments depends on a knowledge of the flow within the cavity. The present report is addressed to this problem of the cavity dynamics and will propose a new experimental diagnostic to directly measure the Mach number in the cavity.

As background let us now discuss the present evidence for the flow conditions within this cavity. From the analysis of the experimental data by Ripin et al.[3], it appears that the shock front and attendent high density shell expand like

$$R_s(\mathrm{cm}) = 0.123\ \left[\frac{E(J)}{P_o(T)}\,\frac{\mu(N_2)}{\mu}\right]^{0.2}\ t^{\,0.4}\ (\mathrm{nsec}) \qquad (1)$$

Manuscript approved July 15, 1985.

where R_s is the shock radius in cm, E is the laser energy in Joules, p_o is the ambient pressure in Torrs, μ is the mean molecular weight, and t is the time in nsec. This formula has exactly the same functional dependencies as the spherical, adiabatic, expansion of a Taylor-Sedov self-similar blast wave.[5] In this ideal theoretical model and for a ratio of specifc heat (γ) between 1 and 3, the density decreases and the temperature increases toward the center in such a way that the pressure is roughly constant, while the velocity decreases nearly linearly with radius inward. If electron thermal conduction is important the adiabatic assumption can be replaced by an isothermal one in the extreme limit. In this case the expansion is still self-similar, with again the functional form of eqn (1), but the interior temperature is that of the shock front and the density and velocity decrease toward the center.[6]

The condition for applicability of the self-similar, Taylor-Sedov solution to an explosion has generally been that the initial conditions are forgotten. This can be translated into the statement that the mass swept up by the shock front ($M_{sw} = 4\pi\rho_o R_s^3/3$, where ρ_o is the ambient density) be much larger than the debris mass (M_d). Detailed numerical simulations by Gull[7] show that by the time $M_{sw}/M_d \sim 10$ the outer region of the cavity resembles the Taylor-Sedov blast wave solution while the inner region does so by the time $M_{sw}/M_d \sim 50$. In the experiment a typical target mass is 4μgr but only ~ 0.3μgr are ablated to become debris. Using the relation

$$\rho_o(\mathrm{gr/cm^3}) = 1.6 \times 10^{-6}\ p_o(T)\ \frac{\mu(N_2)}{\mu} \qquad (2)$$

at standard temperature, one finds for $p_o = 5$ Torr that $M_{sw}/M_d = 10$ at $R_s \sim 0.45$ cm, and $M_{sw}/M_d = 50$ at $R_s \sim 0.76$ cm. For reference at 23 Joules of laser energy the corresponding times are 12 nsec and 44 nsec, respectively. Shadowgraph observations typically lie within 55 to 155 nsec.

Given the above two facts for the high pressure runs; vis., (i) that the blast wave radius follows the Taylor-Sedov relation, and (ii) that the ratio $M_{sw}/M_d \gg 1$ at $R_s \sim 1$ cm, one is led to conclude that the flow within the cavity follows the adiabatic (or isothermal) Taylor-Sedov solution. Consequently, the cavity should be at least as hot as the shock front. However, recent numerical calculations of the experiment by Stellingwerf[8] predict a quite different picture. Using the same parameters mentioned above ($p_o = 5$ Torr of N_2 and E_o =23 Joules), he found that the temperature

decreases from the swept-up shell back into the interior, i.e., a cold cavity, even as late as 64 nsec. He finds no evidence that the solution is evolving toward the Taylor-Sedov blast wave, although the blast wave radius does agree with the $t^{2/5}$ dependence of eqn. (1). The reason for the discrepancy from the Taylor-Sedov blast wave is not obvious from the calculation. It is noteworthy that the reflected shock, which forms at one equal mass radius, fails to move back into the cavity and heat it as would be expected in the approach to the Taylor-Sedov solution. In any case it is clear that the prediction of a cold cavity is in complete variance with the Taylor-Sedov model.

Unfortunately, there are no direct experimental observations on the temperature of the cavity to distinguish between the two above models. Spectroscopy could in principle measure the thermodynamic state in the cavity but the measurements would be severely hampered by the strong continuum from the swept-up shell. In one shot (#14197) a large wedge was placed so that it protruded into the cavity by 155 nsec. The original intent was to see if the aneurism was affected (it wasn't). The resulting non-stationary oblique shocks seen in the dark-field shadowgraph are interesting, but the configuration of the shocks and wedge was so complex that any conclusion based on the shock geometry is highly tentative.

Taking off from this idea, though, we suggest the use of small obstacles, such as spheres or conical bullets, to directly probe the cavity. Consider the sequential interaction of a moving shock front with a sphere fixed in the lab frame as depicted in Fig. 1. As the main shock wave engulfs the obstacle a reflected shock is formed and meets the main shock at the triple points.[9] Further into the sequence the reflected shock expands away from the obstacle and the main shock reforms downstream. At this point the obstacle is subject to the postshock flow, which relative to the main shock is subsonic, but may be subsonic or supersonic relative to the obstacle. Let M_1 be the Mach number of the postshock flow relative to the obstacle. If M_1 is < 1 the reflected shock continues to move upstream of the obstacle and degrades into a sound wave. If $M_1 > 1$, a standoff bow shock is formed, as shown in the last sequence of Fig. 1. In this case, classical gas dynamics provides a quantitative relation between the standoff distance and the Mach number M_1. Thus once an obstacle is engulfed by the expanding cavity, the absence or presence of a bow shock and its standoff distance can indicate the local Mach number. To go from here to a local temperature, an assumption of the velocity

and ratio of specific heat is required. Since both the Taylor-Sedov solution and Stellingwerf's calculation have a nearly linearly velocity profile, the use of a linear velocity law for the experimental data is reasonable. Actually, the procedure could be reversed to provide a further test on the theoretical and numerical models; from the calculated Mach number of a numerical model the standoff distance of a bow shock from a small obstacle could be predicted and compared with experimental observations.

We present a cursory review of the gas dynamic theory for standoff bow shocks in section II. The main results are presented in Figures 5a and 5b. The applicability of the theory to the experiment is discussed in section III. There we first list the assumptions behind the simple theory and the complications in the experiment Then we note that it would be useful to study the temporal evolution of the standoff distance as a gross analysis of the cavity dynamics. This approach is exemplified by discussing the problem for the adiabatic and isothemal self-similar blast waves, for Stellingwerf's model, and for a recent numerical model developed at NRL. Section IV contains a summary with the major conclusions.

II. ANALYSIS

The theoretical analysis to determine the standoff distance of a bow shock cannot be reduced to a single equation, but is instead composed of several separate steps. We will not present each step in complete detail for the basic procedure is outlined in several sections of A.H. Shapiro's text on gas dynamics.[10] Our approach will be to gather the separate steps into an organized sequence, derive or quote the main equations, and discuss our method of solution. Shapiro's results are obtained for a ratio of specific heat γ equal to 1.4 since the problem was first solved in aeronautics. We will present results for $\gamma = 1.2$ and 5/3 to explicitly demonstrate the dependency on γ. This range is considered for the γ of the cavity is unknown: at the main shock where there are rapid chemical reactions $\gamma = 1.2$, while if there are no internal degrees of freedom $\gamma = 5/3$.

A. Maximum turning angle at an oblique shock

The first step is to determine the maximum turning angle a streamline of incident Mach number M_1 can undergo upon passing through an oblique shock.

The jump relations for a perfect gas across an oblique shock can most easily be obtained from the normal shock relations by letting $V_1 \to V_1 \sin\phi$ and $V_2 \to V_2 \sin(\phi - \chi)$, , where the geometry and nomenclature are contained in Figure 2. This amounts to rewriting the standard relations in terms of the normal velocity components. One then finds

$$\frac{\rho_2}{\rho_1} = \frac{V_1 \sin\phi}{V_2 \sin(\phi-\chi)} = \frac{(\gamma + 1)M_1{}^2 \sin^2\phi}{(\gamma-1)M_1{}^2 \sin^2\phi + 2}, \tag{3}$$

$$\frac{p_2}{p_1} = \frac{2\gamma M_1{}^2 \sin^2\phi}{\gamma + 1} - \frac{\gamma - 1}{\gamma + 1}, \tag{4}$$

$$M_2{}^2 \sin^2(\phi - \chi) = \frac{2 + (\gamma - 1)\, M_1{}^2 \sin^2\phi}{2\gamma M_1{}^2 \sin^2\phi - (\gamma - 1)}, \tag{5}$$

and the continuity of the tangential velocity component is

$$V_1 \cos\phi = V_2 \cos(\phi - \chi). \tag{6}$$

By combining relations (3) and (6) one readily finds

$$\cot(\phi - \chi) = \cot\phi \, \frac{(\gamma + 1)\, M_1{}^2 \sin^2\phi}{(\gamma - 1)\, M_1{}^2 \sin^2\phi + 2} \tag{7}$$

from which

$$\cot\chi = \tan\phi \left[\frac{(\gamma + 1)\, M_1{}^2}{2(M_1{}^2 \sin^2\phi - 1)} - 1\right] \tag{8}$$

A relation which will be needed later is obtained from eqns. (5) and (7):

$$M_2{}^2 = \frac{2 + (\gamma - 1)\, M_1{}^2}{2\gamma M_1{}^2 \sin^2\phi - (\gamma - 1)} + \frac{2M_1{}^2 \cos^2\phi}{2 + (\gamma - 1)\, M_1{}^2 \sin^2\phi}. \tag{9}$$

From eqn (8) one finds, in a plot of χ versus ϕ, that a line of constant M_1 begins at $(\chi, \phi) = [0, \arcsin(1/M_1)]$ corresponding to a Mach wave, increases to a maximum χ_{max} at ϕ_{max} , and then ends at $(\chi, \phi) = (0, \pi/2)$ corresponding to normal shock. The value of χ_{max} can be found by differentiating eqn (8) with respect to ϕ and solving for ϕ_{max} :

$$\sin \phi_{max} = [\frac{1}{4\gamma M_1^2}\{(\frac{\gamma + 1}{2}M_1^2 - 2) +$$

$$[(\frac{\gamma + 1}{2}M_1^2 - 4)^2 + 4\gamma(1 + \frac{\gamma + 1}{2}M_1^2)]^{1/2}\}]^{1/2} \qquad (10)$$

The value of χ_{max} is then given by eqn. (8). For a given free stream Mach number M_1, $1/M_1 < \sin \phi \le \sin \phi_{max}$ is the range of allowable ϕ for the so-called weak shock solution. The strong shock solution, wherein $\phi > \phi_{max}$, are not observed in the laboratory but are indicative of shock detachment from a cone or wedge.

B. Supersonic flow past a cone.

We next need to solve for the flow past a cone in a normal incidence supersonic stream of Mach number M_1. Given that the flow between the standing, attached, conical shock and the cone's surface is steady, adiabatic, and irrotational, the gas dynamic equations can be reduced to a pair of ordinary differential equations. The flow is conical, i.e., dependent only on the angle θ of Figure 2. The derivation is given by Shapiro[10] on page 654 in a spherical coordinate system with velocity components V_r and V_θ at an arbitrary point P. In our notation the equations become

$$\frac{d^2U}{d\theta^2}\left[\frac{\gamma + 1}{2}\left(\frac{dU}{d\theta}\right)^2 - \frac{\gamma - 1}{2}(1 - U^2)\right]$$

$$= (\gamma - 1)\, U\, (1 - U^2) + \frac{\gamma - 1}{2}(1 - U^2)\frac{dU}{d\theta}\cot\theta$$

$$-\gamma U\left(\frac{dU}{d\theta}\right)^2 - \frac{\gamma - 1}{2}\left(\frac{dU}{d\theta}\right)^3\cot\theta, \qquad (11)$$

and

$$V_\theta = \frac{dV_r}{d\theta}. \qquad (12)$$

Here $U = V_r/V_{max}$ and V_{max} is the maximum velocity for a given stagnation temperature. It is related to the adiabatic sound speed through

$$c^2 = \frac{\gamma - 1}{2}(V_{max}^2 - V^2),$$

and hence, in terms of a local Mach number,

$$\frac{V^2}{V_{max}^2} = \frac{(\gamma - 1)M^2}{2 + (\gamma - 1)M^2}.$$

Equation (11) was first derived by Taylor and Maccoll[11] in 1933 and they found excellent agreement between their solution and laboratory experiments. Their method of solution, described in Shapiro, begins at the cone surface and is cumbersome given modern day computers. Instead we employ the following method. For a chosen γ, M_1, and ϕ, eqns, (8) and (9) give the turning angle χ and the immediate postshock Mach number M_2. From eqn. (13) one gets V_2^2/V_{max}^2 and the velocity components at the shock front, where $\theta = \phi$, are

$$\frac{V_r}{V_{max}} = \frac{|V_2|}{V_{max}} \cos(\phi - \chi) = U,$$

and

$$\frac{V_\theta}{V_{max}} = - \frac{|V_2|}{V_{max}} \sin (\phi - \chi).$$

Finally from eqn (12) one has $dU/d\theta$, and eqn (11) can be integrated starting at the shock in the decreasing θ-direction till $dU/d\theta = 0$. Since this last relation means $V_\theta = 0$, it represents the inner boundary condition on the cone surface and the corresponding angle θ is the half angle δ of the cone.

The results for $\gamma = 1.2$ and 5/3 are presented in Figures 3a and 3b, respectively. The upper dashed line in each graph is the maximum shock angle ϕ_{max} for a given free stream Mach number M_1. Along this line the starting conditions for the integration of eqn. (11) correspond to the solution for the maximum turning angle χ_{max} discussed in the previous subsection. Consider a cone at a fixed half angle δ, i.e., a solid line. As M_1 decreases the shock angle ϕ increases until ϕ_{max} is reached. Further reduction of M_1 leads to a detached bow shock in front of the cone. We note that the solid lines for large δ show the largest variation for the different γ's, while near the Mach wave ($\sin \phi = 1/M_1$), the difference is small. It is also true that the small angle cones lead to very weak oblique shocks with small density jumps.

Another way of presenting the results on the maximum shock angle is given in Figure 4. Here the maximum half angle δ_{max} for an attached shock on a cone is plotted as a function of the free stream Mach number M_1 (solid lines). The corresponding angles for a two-dimensional wedge are shown as dashed lines. The latter results are simply obtained from eqns. (8) and (10) since $\delta_{max} = \chi_{max}$ for a wedge. The large difference between a wedge and cone in Figure 4 clearly indicates a strong dependence on the geometry of the obstacle,

C. Standoff distance for a detached bow shock

The stage is now set for computing the standoff distance for a detached bow shock in front of a sphere or a cone with $\delta > \delta$ max. The approximate procedure is given by Shapiro[10] starting on page 884. Since there are many substeps and Shapiro's description is fairly complete we will not repeat it here. We do mention several items. First, the method requires the determination of the sonic point on the surface of the sphere which depends upon a knowledge of δ_{max} for a cone derived in the last subsection. Second, the method requires the shock angle ϕ_s for which the downstream flow is exactly sonic. This can be determined from eqn. (9) by setting $M_2 = 1$ and solving for $\sin \phi_s$;

$$\sin \phi_s = [\frac{1}{2\gamma M_1^{\,2}(1 + a)}\{a^2 - 1 + M_1^{\,2}(\gamma + a^2) +$$

$$+ [a^2 - 1 + M_1^{\,2}(\gamma + a^2))^2 + 4\gamma(1 + a)^2]^{1/2}\}]^{1/2},$$

where $a = (\gamma - 1)/2$. Third, eqn. (22.8) of Shapiro is not apparent but can be derived using his notation as follows:

$$\frac{\rho_s V_s}{\rho_\infty V_\infty} = \frac{(p_s/T_s)\, M_s C_s}{(p_\infty T_\infty)\, M_\infty C_\infty} = \frac{p_s}{p_\infty}\sqrt{\frac{T_\infty}{T_s}}\,\frac{1}{M_\infty}$$

$$= \frac{p_{oc}}{p_{o\infty}}\,\frac{1}{M_\infty}\,[(\frac{2}{\gamma + 1})\,(1 + \frac{\gamma - 1}{2}\,M_\infty^{\,2})]^{\frac{\gamma + 1}{2(\gamma - 1)}},$$

where we have used $M_s = 1$, the isentropic relations for a perfect gas,

$$p_s = p\left(1 + \frac{\gamma - 1}{2} M^2\right)^{\frac{\gamma}{\gamma - 1}}$$

$$T_o = T\left(1 + \frac{\gamma - 1}{2} M^2\right),$$

and the fact that the stagnation (subscript o) temperature does not change across a shock. (The subscript ∞ denotes free stream conditions, subscript s denotes sonic line conditions, and subscript c denotes centroid streamlines values). The ratio $p_{oc}/p_{o\infty}$ can be obtained by using eqn. (4) for the centroid streamline at the shock front and then applying the isentropic relations for a perfect gas. Fourth, as Shapiro notes, the method indicates that the shape of the obstacle's nose upstream of the sonic point is not important in determining the shock location.

The outcome of the procedure gives the ratio of the standoff distance to the height of the sonic point on the body. The result can easily be converted to more practical distances through geometrical conditions depending on the body shape. The solution for a sphere and a conical bullet are presented in Figures 5a and 5b, respectively. We emphasize that the results for a cone are only applicable if the cone half angle δ is larger than the δ_{max} from Figure 4. In going from an experimentally observed L/d to a Mach number, the resulting M_1 is quite sensitve to γ for small L/d. In going the other direction, i.e., starting from a given M_1, the predicted L/d is not very sensitive to γ. It is also clear that the ratio L/d is not discriminating for large M_1.

Finally, we note that comparison of the results for the case $\gamma = 1.4$ with experiments is summarized by Shapiro and shows good agreement. In addition, a natural question which arises is how soon after the main shock collides with the obstacle is the above method applicable. We have employed the above method to the last two photographs in Bryson and Gross[9] which show the shock-sphere interaction in stage three of Figure 1. We find an upstream Mach number relative to the sphere of 1.5-1.6, while the actual Mach number is slightly less, i.e., 1.333. (The actual value was obtained from the quoted incident Mach number in the Bryson and Gross experiment and the shock jump relations).

III. Applicability to the Experiment

As described in the Introduction, we are proposing that a small obstacle in the upgraded experiment be used to probe the nature of the cavity. The flow Mach number may then be estimated from the standoff distance of the bow shock and Figures 5a and 5b. It is important to emphasize that the relevent interaction is that of the obstacle with the flow in the cavity and not the interaction of the main shock with the obstacle. In the latter case the Mach number of the main shock is large while in the former the Mach number is reduced since the cavity temperature is probably hotter than that of the ambient material and the gas velocity is smaller than the shock front. In general, the smaller the Mach number the larger the variation in the geometrical configuration of the shock interaction, and hence the easier it is to predict and obtain information on the flow. We further suggest that the standoff distance of a bow shock about a fat cone or sphere be studied rather than the attached shock on a cone. In the latter case, Figures 3a and 3b show that it is only for narrow cones that a large range in M_1 is allowed, but for these type of obstacles the density jump across the oblique shock is weak and it may be difficult to detect with shadowgraphy techniques.

There are, however, several caveats that need to be considered before the theory can be employed. According to section II, the essential assumptions behind the theoretical development were that the upstream flow was uniform and that the flow on each side of the shock was steady and adiabatic.

Clearly, for an obstacle in the cavity of the experiment, the upstream flow is not uniform but diverging since the blast wave expansion is more nearly spherical than planar. Likewise the flow is not steady. Both of these objections may be somewhat alleviated by using small spheres in the sense that d/D is small, where d is the obstacle's diameter and D is the distance of the obstacle from the target. Spheres are better than cones for the uniform problem since one need not worry about alligning the cone center line with the flow direction. As long as the gradient length scales of the flow variables are large compared to d and the temporal scale is long compared to the flow transit time, the problem of unsteady flow is also manageable. We will have more to say about rapidly changing flows at the end of this section.

The adiabaticity of the cavity flow is also questionable. If the cavity temperature T_c is hot, electron thermal conduction may be important and a two fluid description could be more appropriate for the cavity. This leads directly to the problem that if T_e is large (or the cavity density is low enough) the mean free path in the cavity could become larger than a small obstacle. An example of this case is that of the Moon in the supersonic solar wind which shows no bow shock. It should be noted though, that for the theoretical and numerical models presented on the experiment, either the cavity is so hot that the flow is mostly subsonic, in which case there is no bow shock, or the cavity is cold and the adiabatic approximation is reasonable.

There is a further subtle problem mentioned by B. Ripin[12] which would be associated with any object in the experimental chamber. When the laser is turned on, the target is heated to such a degree that very energetic photons are emitted. These photons may ionize and heat the surface of an obstacle and may lead to a flow off the obstacle. This in turn would form a boundary layer around the obstacle and change the nature of the shock interaction. At the present time there appears to be no method for testing this or assessing its impact.

Given all the above mentioned problems, and the requirement of an assumed velocity profile to obtain a temperature from the observed Mach number, we suggest that it would still be of interest to place an obstacle in the path of the expanding cavity just to watch the temporal change in the standoff distance of the bow shock. As the cavity expands the fixed obstacle would sample deeper and deeper into the cavity with time. The gross evolution could then be compared with the predictions from theoretical and numerical models. For example, we consider three distinct models for the blast wave. First in Figure 6 we plot the local Mach number for the adiabatic Taylor-Sedov blast wave and the isothermal blast wave as a function of r/R_s where R_s is the radius of the main shock. Since these theoretical solutions are self-similar the Mach number has a self-similar profile. Note that one would expect a bow shock around an obstacle only in the outer 10% of the cavity. Once the obstacle gets inside this region the high temperature and low velocity lead to subsonic flow. For the second model, Figure 7 shows the local adabatic Mach number at two times from Stellingwerf's[8] model "L2NQ." The parameters include

a 25 μm Aℓ target with a 5 Torr background N_2 gas and a laser energy of 23 Joules. The ratio of specific heat γ was evaluated from the specific internal energy ε and the relation $\gamma = 1 + p/\rho\varepsilon$. Note that, contrary to the self-similar models, the Mach number is large throughout the cavity. Finally, the third model is a recent numerical simulation[13] of the experiment which includes the effects of a non-spherical outflow from the target and non-equilibrium chemistry. Details will be presented in a forth coming NRL memo report. Figure 8 shows the Mach number at four different times for the initial conditions of a 4.6 μm thick Aℓ target, situated at x = 0.0 cm , 2.5 Torr background, and 23 Joules of laser energy. The Figure shows that at later times this third model resembles the Taylor-Sedov blast wave in that the front edge moving along the positive x-direction i,e., back toward the laser, is locally supersonic. (The horizontal dashed line marks a Mach number of unity.) The backside has a quite irregular structure though. If an experiment with a stationary obstacle can be constructed, it should be a simple matter to verify which of the competing models are valid.

IV. Summary

We have partially reviewed the method for computing the attached and detached shock geometry for *uniform, steady, adiabatic, supersonic flow* around a blunt obstacle. In Figures 3a and 3b the angle of a conical, attached shock about a cone of half angle δ is plotted against the upstream Mach number M_1. The maximum half-angle δ_{max} for which a cone can support an attached shock is shown in Figure 4. If the conditions for an attached shock are not met, Figures 5a and 5b show the relation between the standoff distance of the detached bow shock, and the upstream Mach number for spheres and conical bullets, respectively.

In this memo report we suggest that a small obstacle, preferably a sphere, be placed in the path of the expanding cavity formed in the NRL Laser/HANE experiment. Then a measurement of the standoff distance of the resulting bow shock can be used with Figure 5 to estimate the local Mach number in the cavity. Assuming a velocity profile for the cavity material, a linear dependence on radius is typical of the models, the proposed diagnostic can provide a rough estimate for the cavity temperature. This physical quantity is unknown at the present time but is clearly relevent for

understanding the relationship between the experiment and a real HANE.

Given that the assumptions listed above in the theoretical treatment of the bow shock geometry may not be rigorously met in the experiment, it would still be of interest to study the temporal evolution of the bow shock standoff distance and compare the observations with predictions from theoretical models. For instance, Figure 6 shows that the flow within the adiabatic and isothermal self-similar blast wave solutions is only supersonic in the outer ~ 10% of the cavity. In the numerical model presented by Stellingwerf (cf. Figure 7) the cavity is supersonic over most of its interior because it is cold, while in the simulation of Giuliani and Mulbrandon (cf. Figure 8) the situation is close to that of the self-similar solutions, at least on the front side. Thus, even given the complications listed in section III on applying the theory to the experiment, in simply detecting a bow shock about an obstacle one could distinguish between completely different models.

Acknowledgments

The experimental group under Dr. Barry Ripin at NRL initially used obstacles to study the blast wave dynamics and I thank Dr. Ripin for several fruitful discussions on refining their idea. I am also grateful to Dr. Bob Stellingwerf of MRC for supplying the run of Mach number versus radius from his model calculations. This research was supported by the Defense Nuclear Agency.

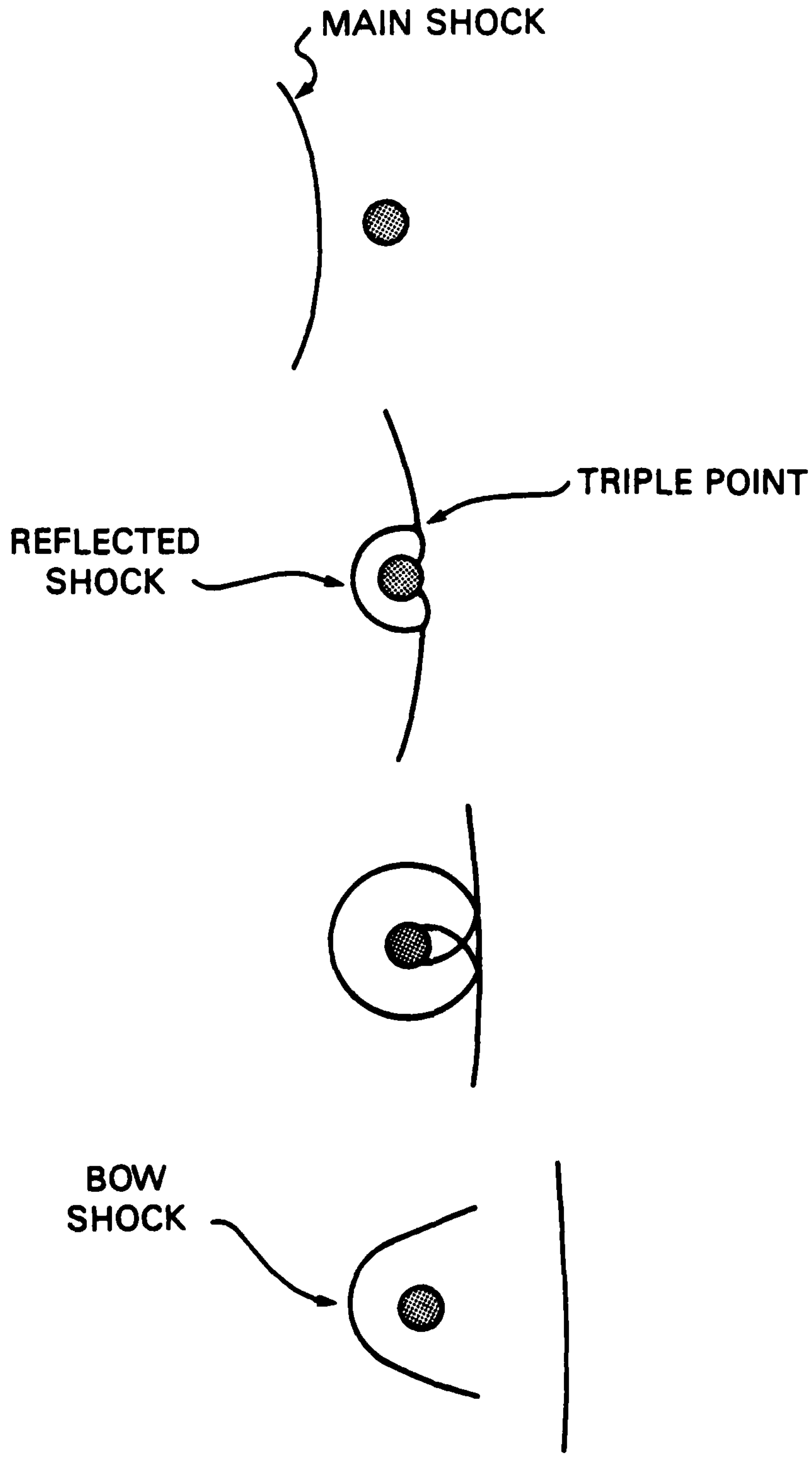

Fig. 1. Schematic diagram of the interactin of a strong shock wave with stationary, spherical obstacle. Time increases downward.

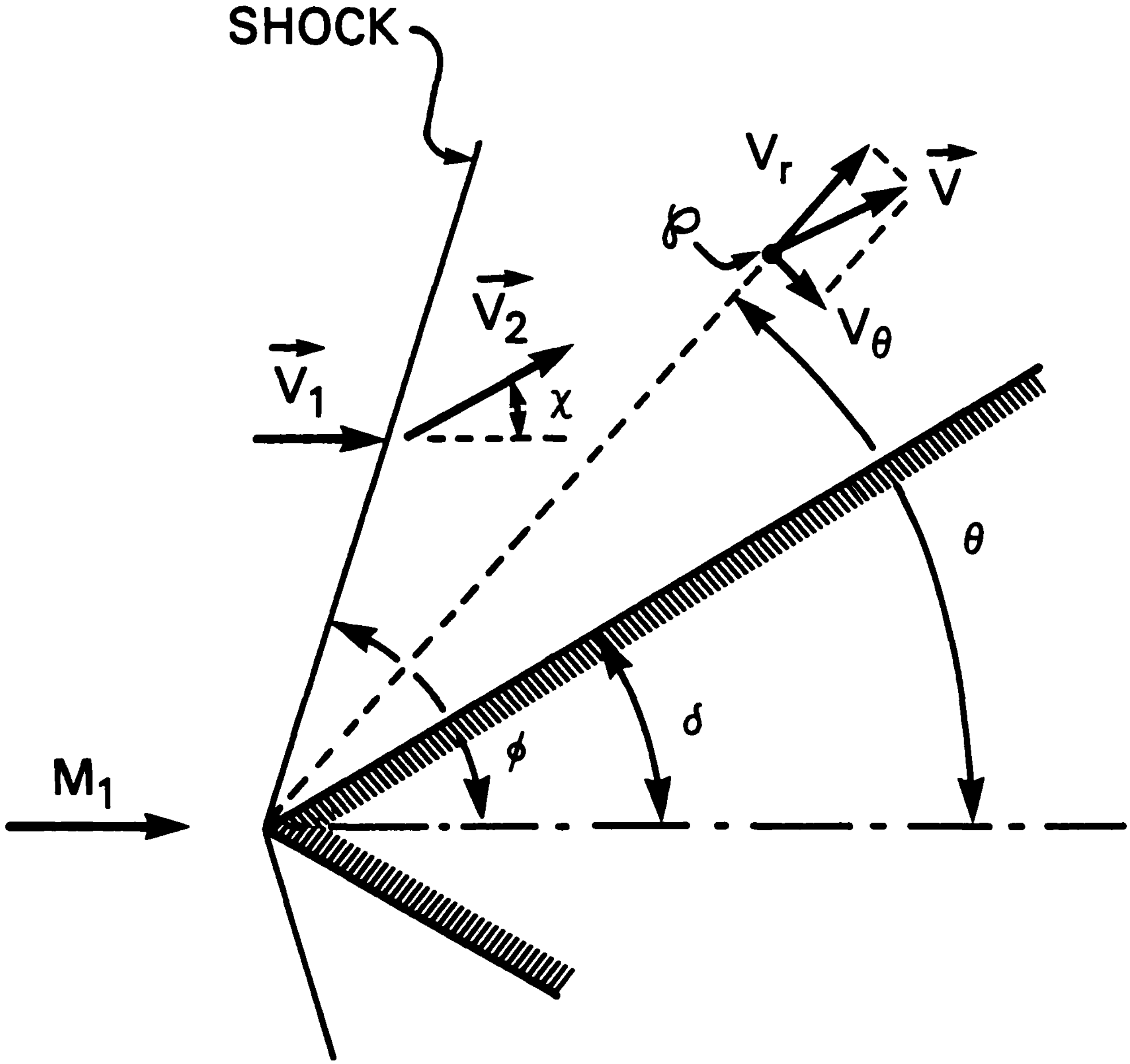

Fig. 2 Geometry and nomenclature used in the analysis of a conical shock about a cone.

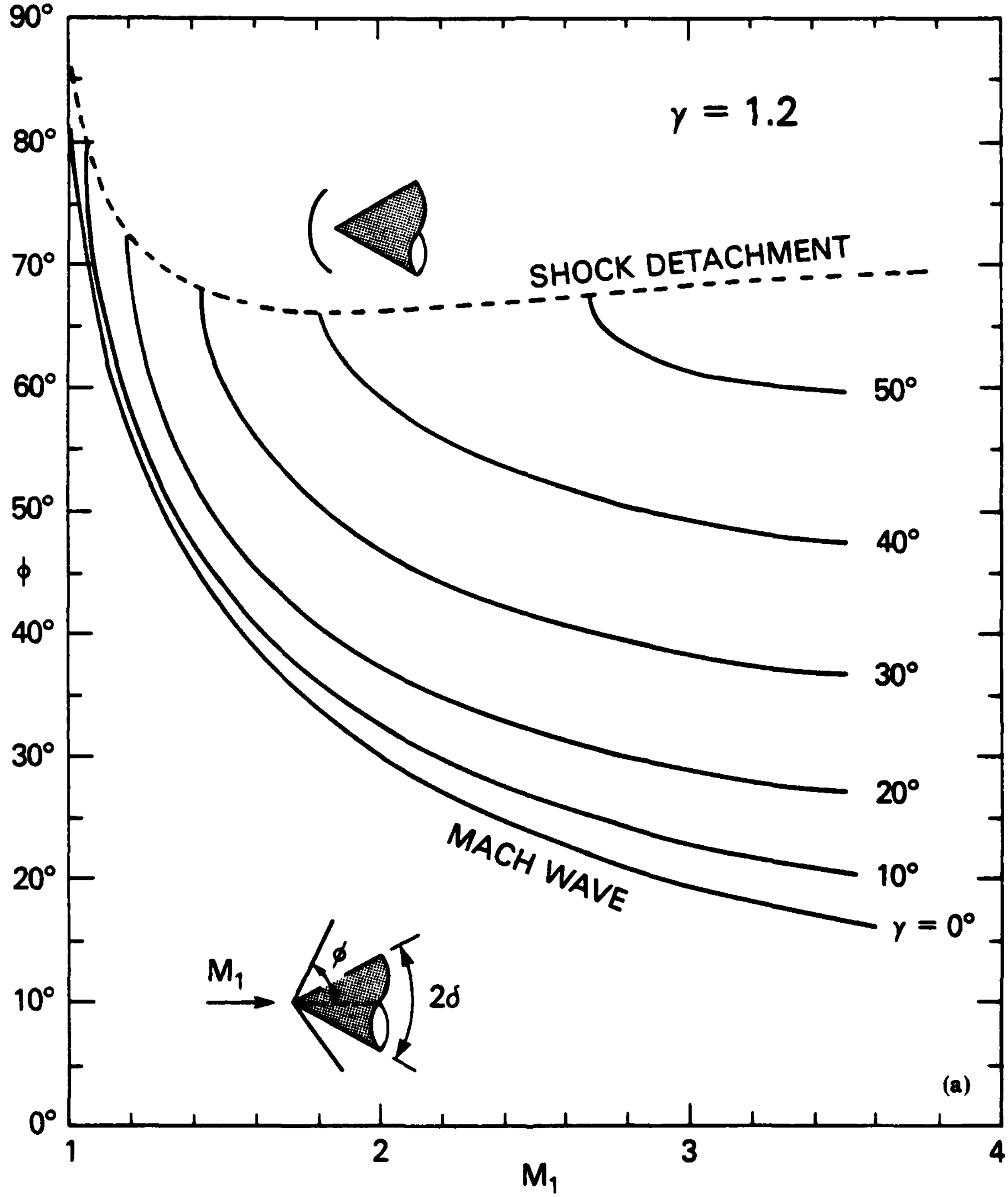

Fig. 3. The shock angle ϕ as a function of the upstream Mach number M_1 for different cones of half angle δ; a) the ratio of specific heat $\gamma = 1.2$, b) $\gamma = 5/3$.

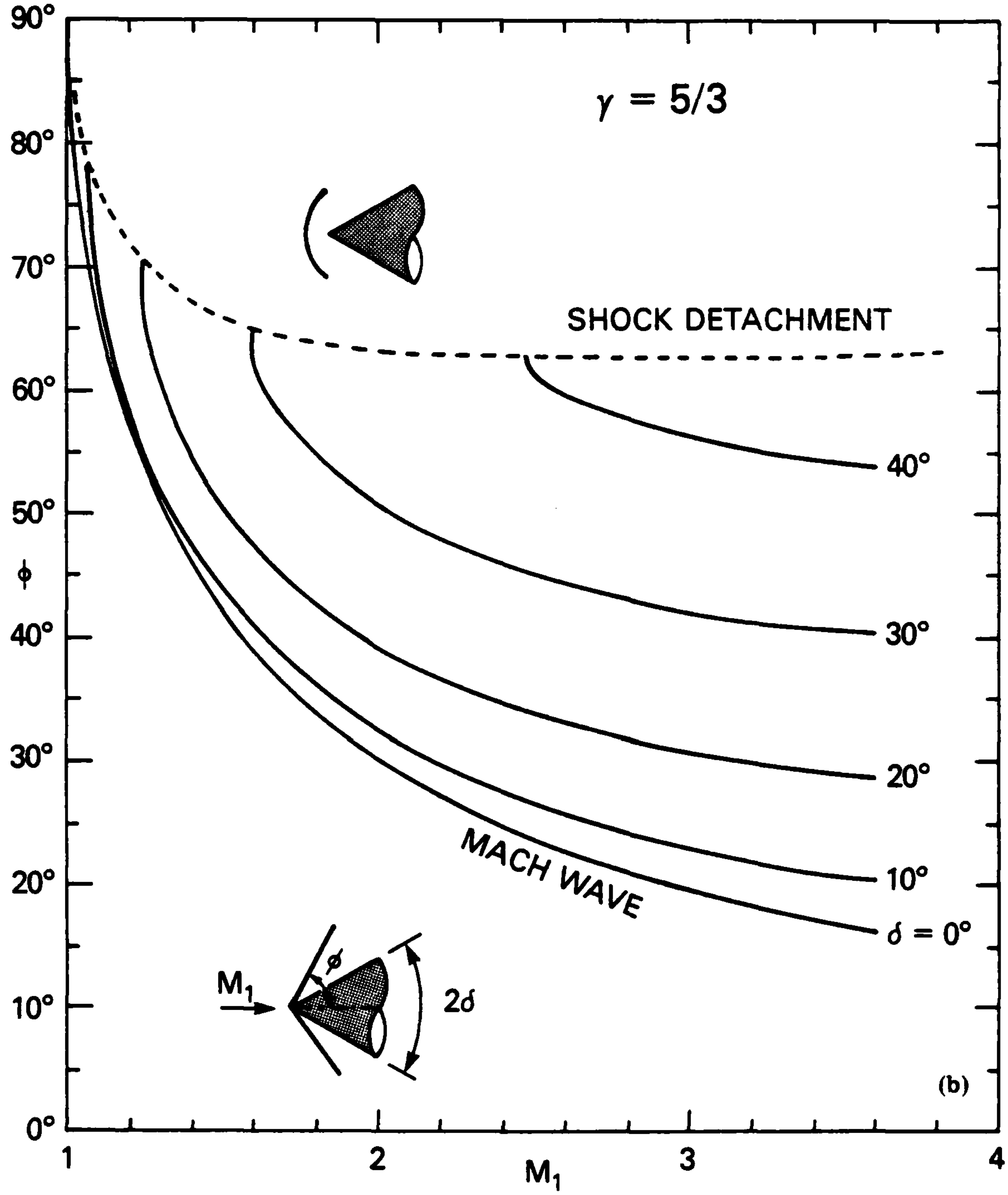

Fig. 3. Cont'd. The shock angle ϕ as a function of the upstream Mach number M_1 for different cones of half angle δ; (a) the ratio of specific heat $\gamma = 1.2$, (b) $\gamma = 5/3$.

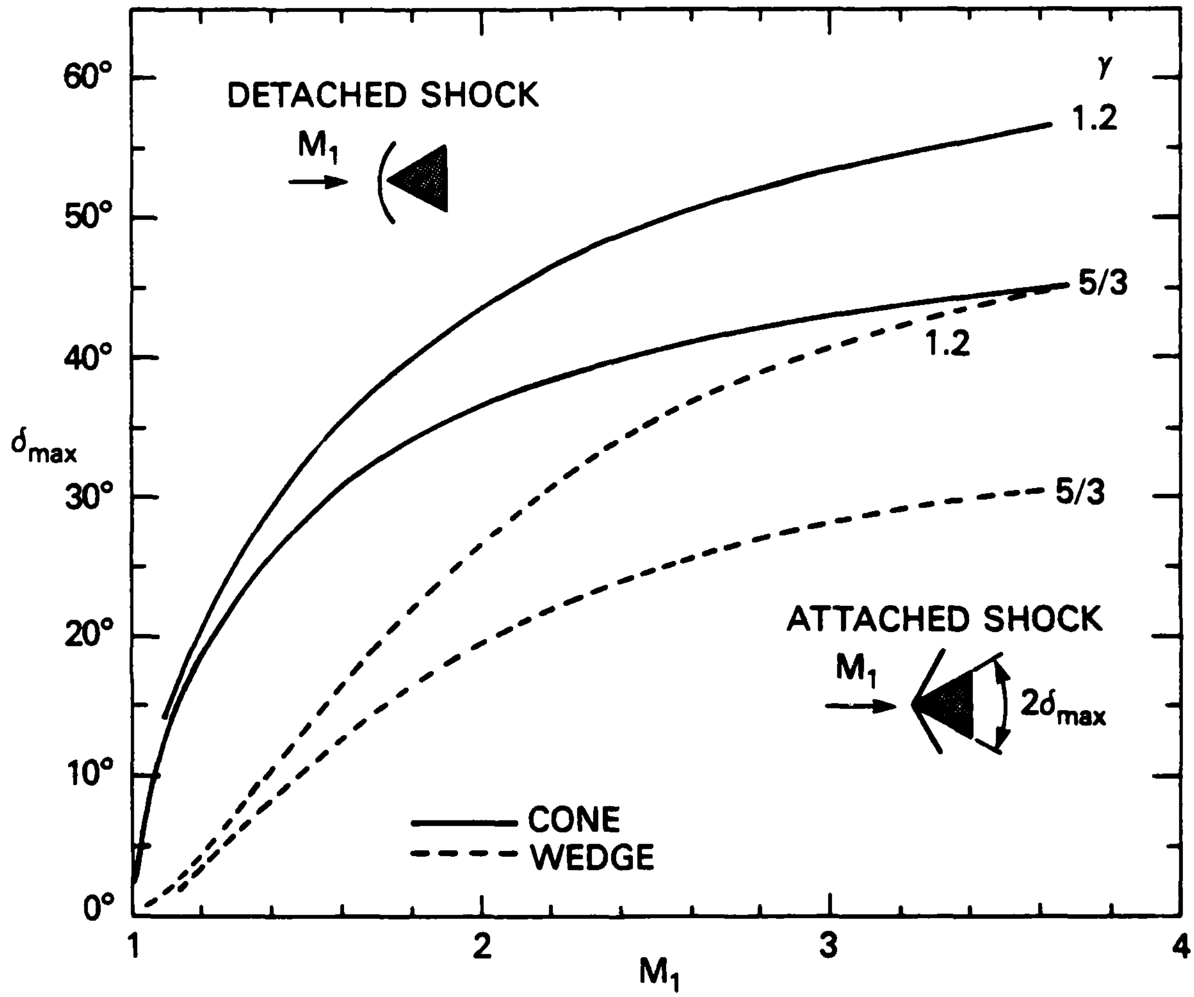

Fig 4. The maximum half angle δ_{max} for which a shock remains attached to a cone (solid lines) or wedge (dashed lines) at the free stream Mach number M_1. Above the line the shock is detached, below attached.

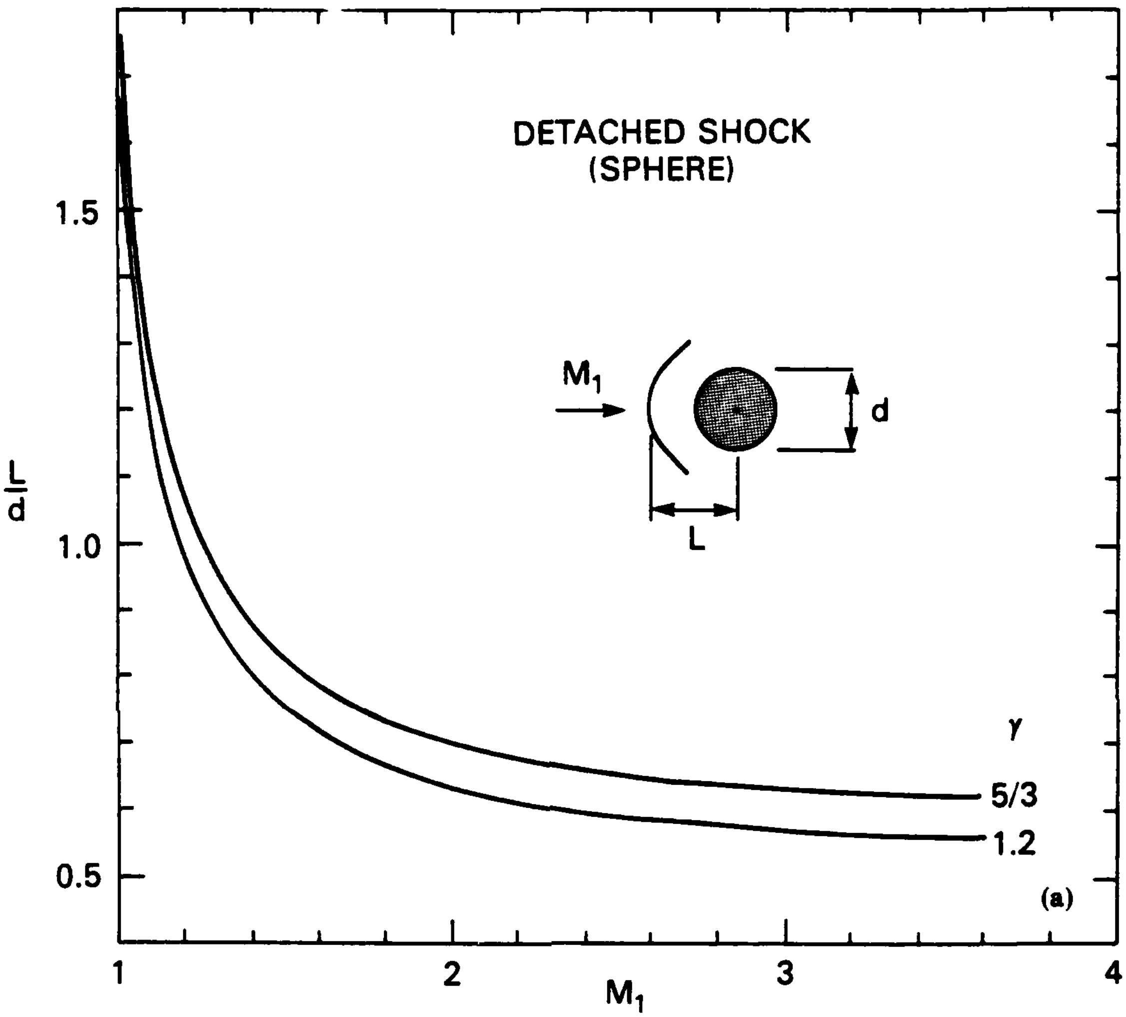

Fig. 5. The relation between the standoff distance of a bow shock, characteristic size of the blunt obstacle, and upstream Mach number; a) sphere, b)conical bullet.

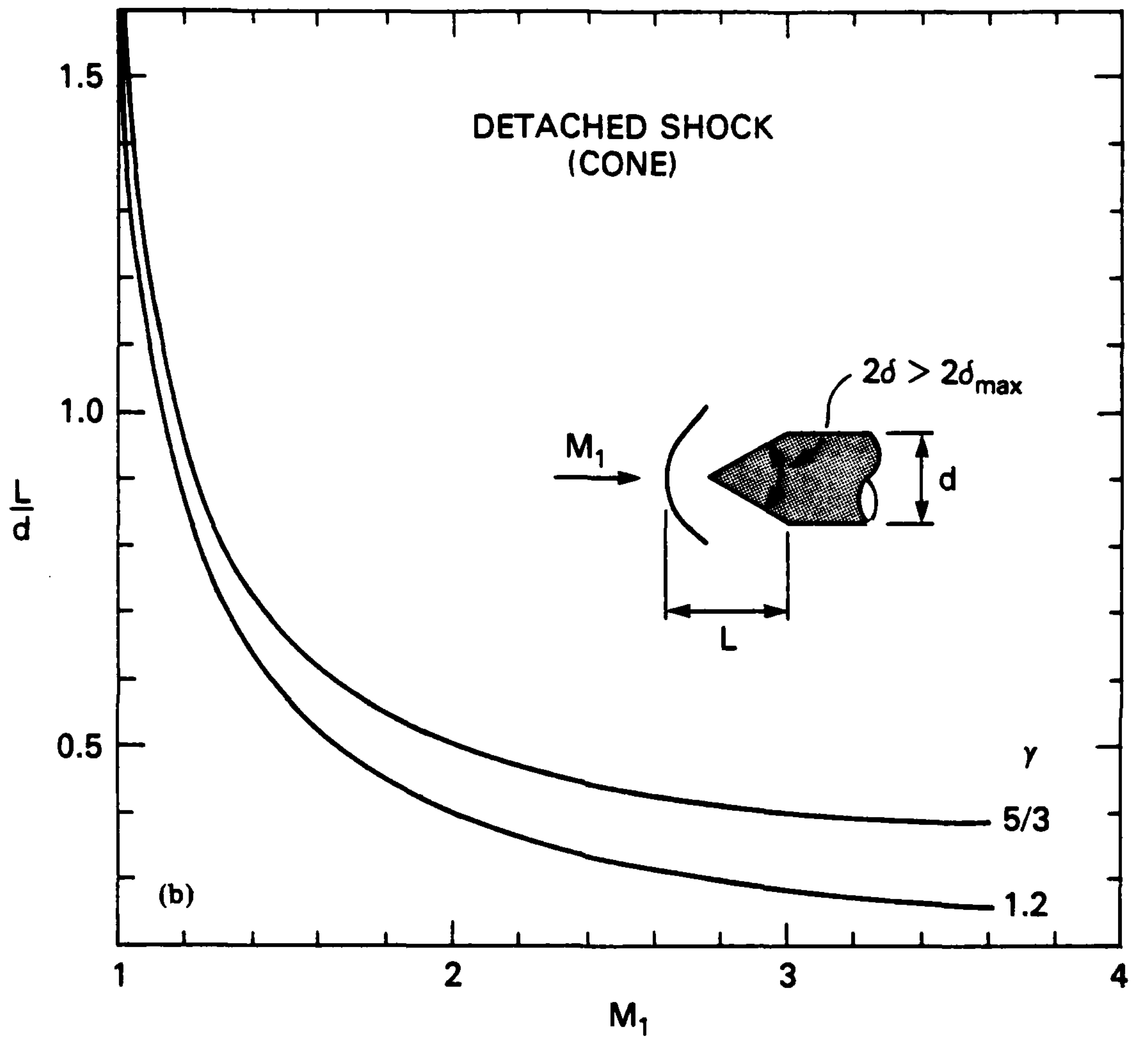

Fig. 5. Cont'd. The relation between the standoff distance of bow shock, characteristic size of the blunt obstacle, and upstream Mach number; (a) sphere, (b) conical bullet.

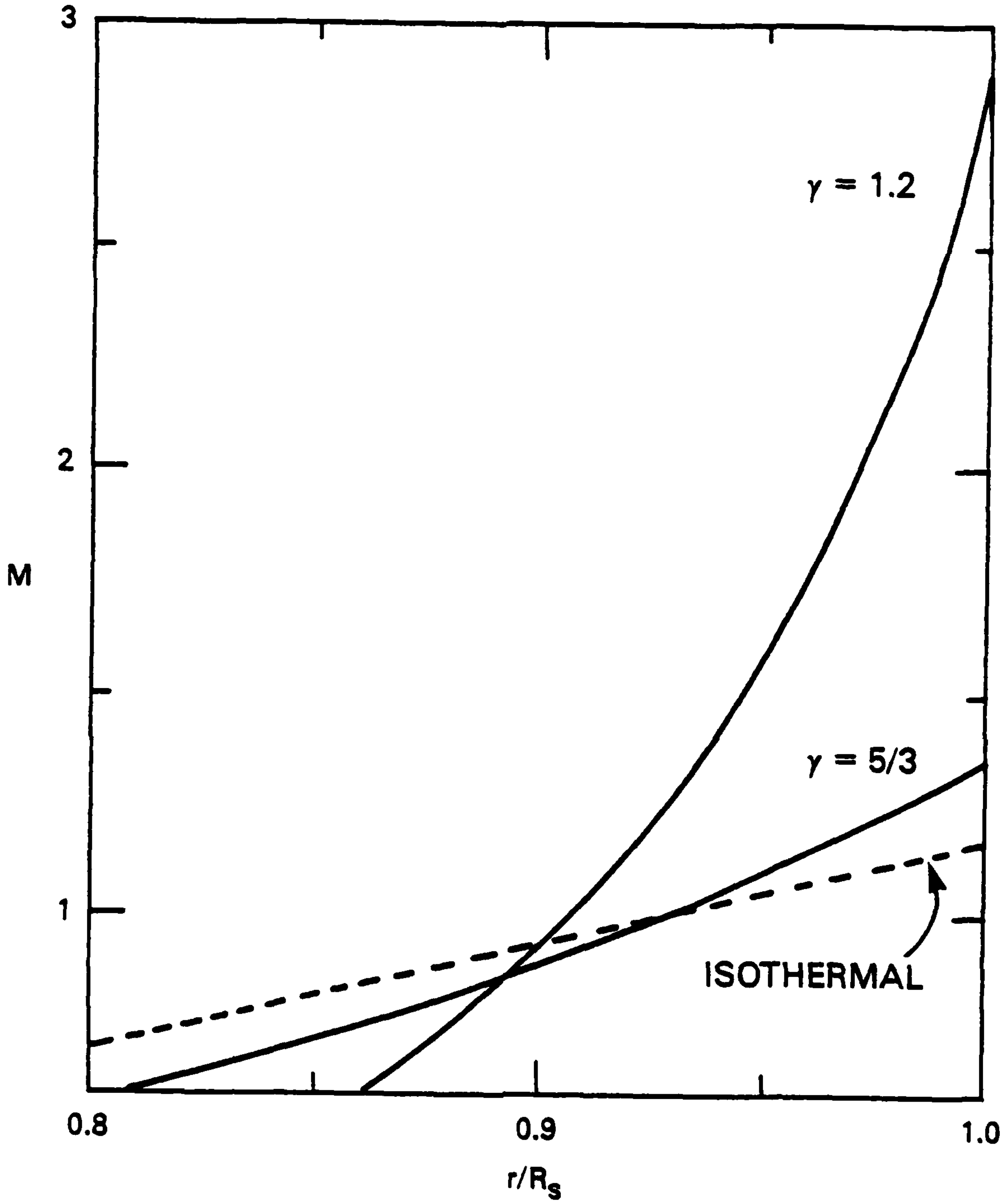

Fig. 6. The local Mach number in the cavity for the adabatic ($\gamma = 1.2$ and $\gamma = 5/3$), self-similar Taylor-Sedov blast wave solution. The self-similar isothermal solution is also shown. R_s is the main shock radius which follows eqn. (1) of the text and r is a spherical coordinate.

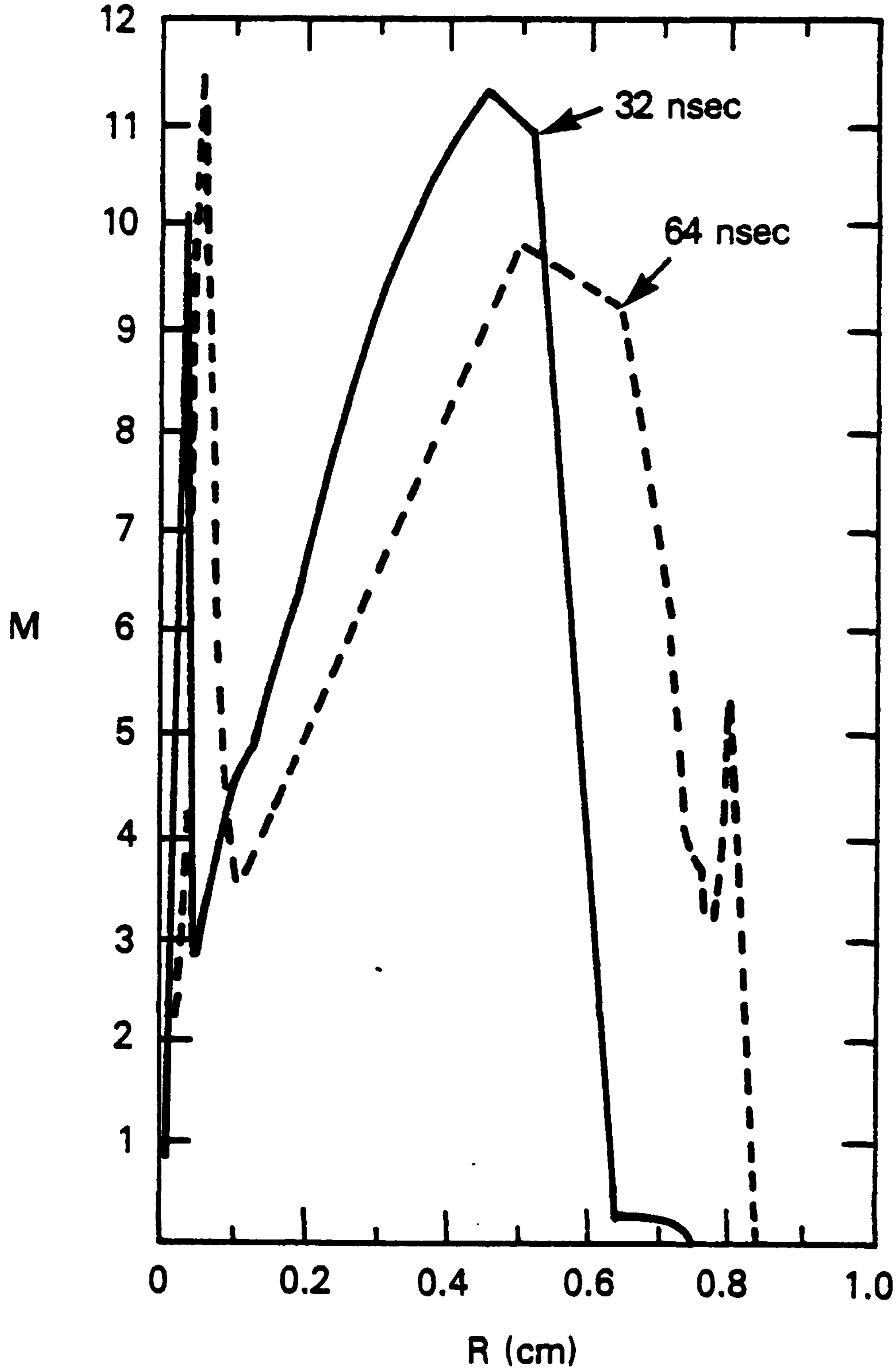

Fig. 7. The local Mach number in the cavity for Stellingwerf's model "L2nQ" shown at two different times. Here R is a spherical radius

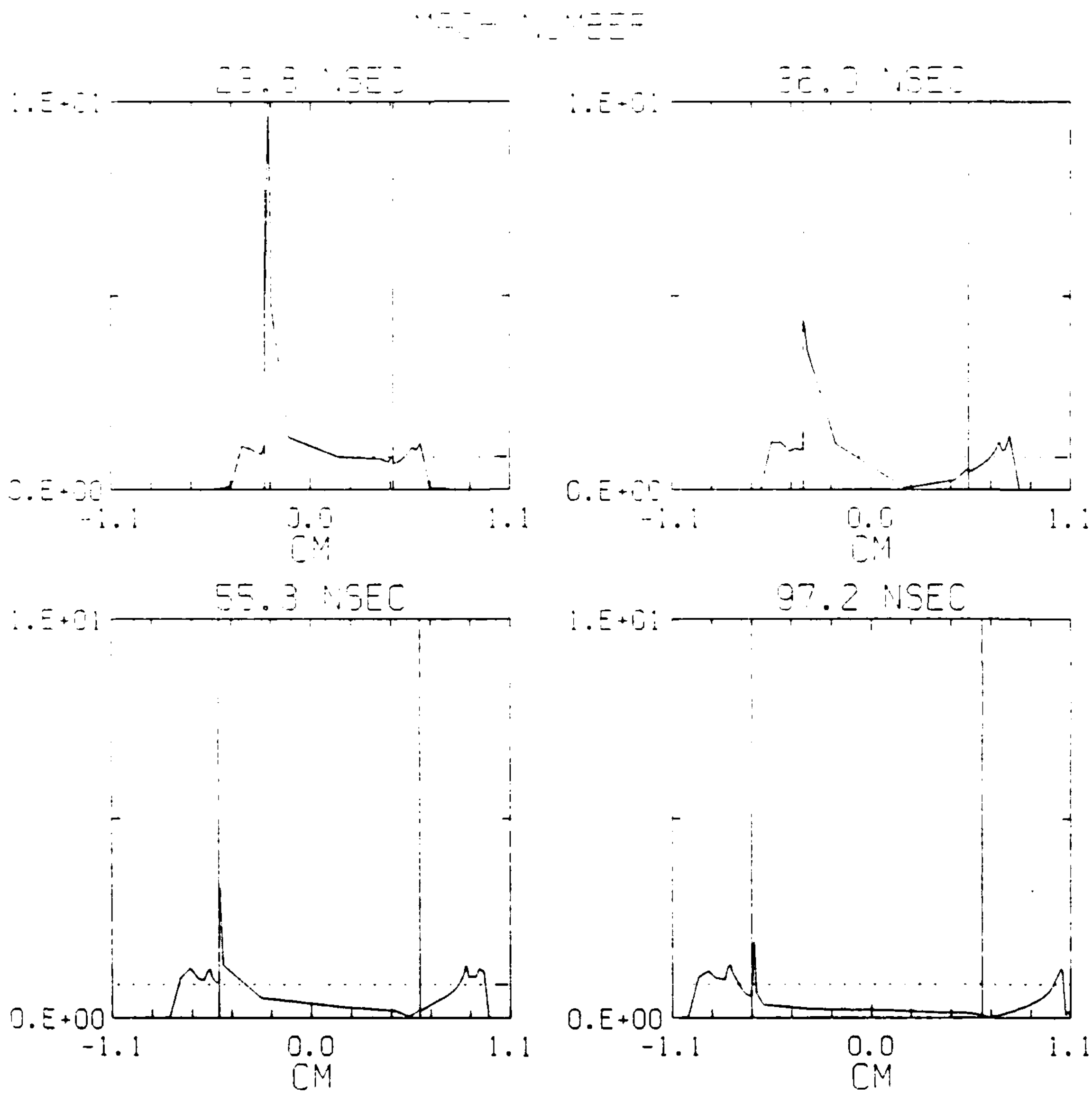

Fig. 8 The local Mach number in the cavity for a numerical model by Giuliani and Mulbrandon. The Aℓ target initially sits at $x = 0$ and expands both toward the laser (at $x = +\infty$) and backwards. The horizontal dashed line marks the Mach number unity and between the vertical lines the gas is all Aluminum, while outside of them the gas is Nitrogen.

References

1. B.H. Ripin, J. Grun, S. Kacenjar, E.A. McLean, and J.A. Stamper, NRL Memo Report #5268, "Introduction to the Laser-Hane Experiment and Summary of Low-Pressure Interaction Results," (1984). **(AD-A138 945)**

2. J.A. Stamper, B.H. Ripin, E.A. McLean, and S.P. Obenschain, NRL Memo Report #5278, "Optical Imaging of a Coupling Region Between Inter-Streaming Plasmas," (1984).

3 B.H. Ripin, J.A. Stamper, and E.A. McLean, NRL Memo Report #5279. "Blast Wave Analysis of High-Pressure Coupling Shells." (1984).

4. J.A. Stamper, "Early-Time High-Altitude Working Group Meeting," held at NRL, November, 1984.

5. L.I. Sedov, Similarity and Dimensional Methods in Mechanics, (Academic Press: New York, 1959).

6. A. Solinger, S. Rappaport, and J. Buff, Ap. J, 201, 381, "Isothermal Blast Wave Model of Supernova Remnants," (1975).

7. S.F. Gull, Monthly Notices Royal Astr. Soc., 161, 47, " A Numerical Model of the Structure and Evolution of Young Supernova Remnants," (1973).

8. R. Stellingwerf, "Early-Time High-Altitude Working Group Meeting," held at NRL, November, 1984.

9. A.E. Bryson and R.W.F. Gross, J. of Fluid Mechanics, 10, 1, "Diffraction of Strong Shocks by Cones, Cylinders, and Spheres," (1961).

10. A.H. Shapiro, The Dynamics and Thermodynamics of Compressible Fluid Flow, Vols, I and II, (Ronald Press Co.: New York, 1954).

11. G.I. Taylor and J.W. Maccoll, Proc. Royal Soc. London (A), 139, 278, "The Air Pressure on a Cone Moving at High Speeds. - I." (1933)

12. B. Ripin, private communication.

13. J.L. Giuliani, Jr. and M. Mulbrandon, "Early-Time High Altitude Working Group Meeting," held at NRL, May, 1985

DISTRIBUTION LIST

DEPARTMENT OF DEFENSE

ASSISTANT SECRETARY OF DEFENSE
COMM, CMD, CONT 7 INTELL
WASHINGTON, D.C. 20301

DIRECTOR
COMMAND CONTROL TECHNICAL CENTER
PENTAGON RM 3E 685
WASHINGTON, D.C. 20301
01CY ATTN C-650
01CY ATTN C-312 R. MASON

DIRECTOR
DEFENSE ADVANCED RSCH PROJ AGENCY
ARCHITECT BUILDING
1400 WILSON BLVD.
ARLINGTON, VA. 22209
01CY ATTN NUCLEAR MONITORING RESEARCH
01CY ATTN STRATEGIC TECH OFFICE

DEFENSE COMMUNICATION ENGINEER CENTER
1860 WIEHLE AVENUE
RESTON, VA. 22090
01CY ATTN CODE R410
01CY ATTN CODE R812

DEFENSE TECHNICAL INFORMATION CENTER
CAMERON STATION
ALEXANDRIA, VA. 22314
02CY

DIRECTOR
DEFENSE NUCLEAR AGENCY
WASHINGTON, D.C. 20305
01CY ATTN STVL
04CY ATTN TITL
01CY ATTN DDST
03CY ATTN RAAE

COMMANDER
FIELD COMMAND
DEFENSE NUCLEAR AGENCY
KIRTLAND, AFB, NM 87115
01CY ATTN FCPR

DEFENSE NUCLEAR AGENCY
SAO/DNA
BUILDING 20676
KIRTLAND AFB, NM 87115
01CY D.C. THORNBURG

DIRECTOR
INTERSERVICE NUCLEAR WEAPONS SCHOOL
KIRTLAND AFB, NM 87115
01CY ATTN DOCUMENT CONTROL

JOINT CHIEFS OF STAFF
WASHINGTON, D.C. 20301
01CY ATTN J-3 WWMCCS EVALUATION OFFICE

DIRECTOR
JOINT STRAT TGT PLANNING STAFF
OFFUTT AFB
OMAHA, NB 68113
01CY ATTN JSTPS/JLKS
01CY ATTN JPST G. GOETZ

CHIEF
LIVERMORE DIVISION FLD COMMAND DNA
DEPARTMENT OF DEFENSE
LAWRENCE LIVERMORE LABORATORY
P.O. BOX 808
LIVERMORE, CA 94550
01CY ATTN FCPRL

COMMANDANT
NATO SCHOOL (SHAPE)
APO NEW YORK 09172
01CY ATTN U.S. DOCUMENTS OFFICER

UNDER SECY OF DEF FOR RSCH & ENGRG
DEPARTMENT OF DEFENSE
WASHINGTON, D.C. 20301
01CY ATTN STRATEGIC & SPACE SYSTEMS (OS)

COMMANDER/DIRECTOR
ATMOSPHERIC SCIENCES LABORATORY
U.S. ARMY ELECTRONICS COMMAND
WHITE SANDS MISSILE RANGE, NM 88002
01CY ATTN DELAS-EO, F. NILES

DIRECTOR
BMD ADVANCED TECH CTR
HUNTSVILLE OFFICE
P.O. BOX 1500
HUNTSVILLE, AL 35807
01CY ATTN ATC-T MELVIN T. CAPPS
01CY ATTN ATC-O W. DAVIES
01CY ATTN ATC-R DON RUSS

PROGRAM MANAGER
BMD PROGRAM OFFICE
5001 EISENHOWER AVENUE
ALEXANDRIA, VA 22333
01CY ATTN DACS-BMT J. SHEA

CHIEF C-E- SERVICES DIVISION
U.S. ARMY COMMUNICATIONS CMD
PENTAGON RM 1B269
WASHINGTON, D.C. 20310
01CY ATTN C-E-SERVICES DIVISION

COMMANDER
FRADCOM TECHNICAL SUPPORT ACTIVITY
DEPARTMENT OF THE ARMY
FORT MONMOUTH, N.J. 07703
01CY ATTN DRSEL-NL-RD H. BENNET
01CY ATTN DRSEL-PL-ENV H. BOMKE
01CY ATTN J.E. QUIGLEY

COMMANDER
U.S. ARMY COMM-ELEC ENGRG INSTAL AGY
FT. HUACHUCA, AZ 85613
01CY ATTN CCC-EMEO GEORGE LANE

COMMANDER
U.S. ARMY FOREIGN SCIENCE & TECH CTR
220 7TH STREET, NE
CHARLOTTESVILLE, VA 22901
01CY ATTN DRXST-SD

COMMANDER
U.S. ARMY MATERIAL DEV & READINESS CMD
5001 EISENHOWER AVENUE
ALEXANDRIA, VA 22333
01CY ATTN DRCLDC J.A. BENDER

COMMANDER
U.S. ARMY NUCLEAR AND CHEMICAL AGENCY
7500 BACKLICK ROAD
BLDG 2073
SPRINGFIELD, VA 22150
01CY ATTN LIBRARY

DIRECTOR
U.S. ARMY BALLISTIC RESEARCH
LABORATORY
ABERDEEN PROVING GROUND, MD 21005
01CY ATTN TECH LIBRARY,
EDWARD BAICY

COMMANDER
U.S. ARMY SATCOM AGENCY
FT. MONMOUTH, NJ 07703
01CY ATTN DOCUMENT CONTROL

COMMANDER
U.S. ARMY MISSILE INTELLIGENCE AGENCY
REDSTONE ARSENAL, AL 35809
01CY ATTN JIM GAMBLE

DIRECTOR
U.S. ARMY TRADOC SYSTEMS ANALYSIS
ACTIVITY
WHITE SANDS MISSILE RANGE, NM 88002
01CY ATTN ATAA-SA
01CY ATTN TCC/F. PAYAN JR.
01CY ATTN ATTA-TAC LTC J. HESSE

COMMANDER
NAVAL ELECTRONIC SYSTEMS COMMAND
WASHINGTON, D.C. 20360
01CY ATTN NAVALEX 034 T. HUGHES
01CY ATTN PME 117
01CY ATTN PME 117-T
01CY ATTN CODE 5011

COMMANDING OFFICER
NAVAL INTELLIGENCE SUPPORT CTR
4301 SUITLAND ROAD, BLDG. 5
WASHINGTON, D.C. 20390
01CY ATTN MR. DUBBIN STIC 12
01CY ATTN NISC-50
01CY ATTN CODE 5404 J. GALET

COMMANDER
NAVAL OCEAN SYSTEMS CENTER
SAN DIEGO, CA 92152
01CY ATTN J. FERGUSON

NAVAL RESEARCH LABORATORY
WASHINGTON, D.C. 20375
  01CY ATTN CODE 4700 S.L. Ossakow,
    26 CYS IF UNCLASS
    (01CY IF CLASS)
    ATTN CODE 4780 J.D. HUBA, 50
    CYS IF UNCLASS, 01CY IF CLASS
  01CY ATTN CODE 4701 I. VITKOVITSKY
  01CY ATTN CODE 7500
  01CY ATTN CODE 7550
  01CY ATTN CODE 7580
  01CY ATTN CODE 7551
  01CY ATTN CODE 7555
  01CY ATTN CODE 4730 E. MCLEAN
  01CY ATTN CODE 4108
  01CY ATTN CODE 4730 B. RIPIN
  20CY ATTN CODE 2628

COMMANDER
NAVAL SPACE SURVEILLANCE SYSTEM
DAHLGREN, VA 22448
  01CY ATTN CAPT J.H. BURTON

OFFICER-IN-CHARGE
NAVAL SURFACE WEAPONS CENTER
WHITE OAK, SILVER SPRING, MD 20910
  01CY ATTN CODE F31

DIRECTOR
STRATEGIC SYSTEMS PROJECT OFFICE
DEPARTMENT OF THE NAVY
WASHINGTON, D.C. 20376
  01CY ATTN NSP-2141
  01CY ATTN NSSP-2722 FRED WIMBERLY

COMMANDER
NAVAL SURFACE WEAPONS CENTER
DAHLGREN LABORATORY
DAHLGREN, VA 22448
  01CY ATTN CODE DF-14 R. BUTLER

OFFICER OF NAVAL RESEARCH
ARLINGTON, VA 22217
  01CY ATTN CODE 465
  01CY ATTN CODE 461
  01CY ATTN CODE 402
  01CY ATTN CODE 420
  01CY ATTN CODE 421

COMMANDER
AEROSPACE DEFENSE COMMAND/DC
DEPARTMENT OF THE AIR FORCE
ENT AFB, CO 80912
  01CY ATTN DC MR. LONG

COMMANDER
AEROSPACE DEFENSE COMMAND/XPD
DEPARTMENT OF THE AIR FORCE
ENT AFB, CO 80912
  01CY ATTN XPDQQ
  01CY ATTN XP

AIR FORCE GEOPHYSICS LABORATORY
HANSCOM AFB, MA 01731
  01CY ATTN OPR HAROLD GARDNER
  01CY ATTN LKB
    KENNETH S.W. CHAMPION
  01CY ATTN OPR ALVA T. STAIR
  01CY ATTN PHD JURGEN BUCHAU
  01CY ATTN PHD JOHN P. MULLEN

AF WEAPONS LABORATORY
KIRTLAND AFT, NM 87117
  01CY ATTN SUL
  01CY ATTN CA ARTHUR H. GUENTHER
  01CY ATTN NTYCE 1LT. G. KRAJEI

AFTAC
PATRICK AFB, FL 32925
  01CY ATTN TN

AIR FORCE AVIONICS LABORATORY
WRIGHT-PATTERSON AFB, OH 45433
  01CY ATTN AAD WADE HUNT
  01CY ATTN AAD ALLEN JOHNSON

DEPUTY CHIEF OF STAFF
RESEARCH, DEVELOPMENT, & ACQ
DEPARTMENT OF THE AIR FORCE
WASHINGTON, D.C. 20330
  01CY ATTN AFRDQ

HEADQUARTERS
ELECTRONIC SYSTEMS DIVISION
DEPARTMENT OF THE AIR FORCE
HANSCOM AFB, MA 01731-5000
  01CY ATTN J. DEAS
    ESD/SCD-4

COMMANDER
FOREIGN TECHNOLOGY DIVISION, AFSC
WRIGHT-PATTERSON AFB, OH 45433
  01CY ATTN NICD LIBRARY
  01CY ATTN ETDP B. BALLARD

COMMANDER
ROME AIR DEVELOPMENT CENTER, AFSC
GRIFFISS AFB, NY 13441
  01CY ATTN DOC LIBRARY/TSLD
  01CY ATTN OCSE V. COYNE

STRATEGIC AIR COMMAND/XPFS
OFFUTT AFB, NB 68113
  01CY ATTN ADWATE MAJ BRUCE BAUER
  01CY ATTN NRT
  01CY ATTN DOK CHIEF SCIENTIST

SAMSO/SK
P.O. BOX 92960
WORLDWAY POSTAL CENTER
LOS ANGELES, CA 90009
  01CY ATTN SKA (SPACE COMM SYSTEMS) M. CLAVIN

SAMSO/MN
NORTON AFB, CA 92409
(MINUTEMAN)
  01CY ATTN MNNL

COMMANDER
ROME AIR DEVELOPMENT CENTER, AFSC
HANSCOM AFB, MA 01731
  01CY ATTN EEP A. LORENTZEN

DEPARTMENT OF ENERGY
LIBRARY ROOM G-042
WASHINGTON, D.C. 20545
  01CY ATTN DOC CON FOR A. LABOWITZ

DEPARTMENT OF ENERGY
ALBUQUERQUE OPERATIONS OFFICE
P.O. BOX 5400
ALBUQUERQUE, NM 87115
  01CY ATTN DOC CON FOR D. SHERWOOD

EG&G, INC.
LOS ALAMOS DIVISION
P.O. BOX 809
LOS ALAMOS, NM 85544
  01CY ATTN DOC CON FOR J. BREEDLOVE

UNIVERSITY OF CALIFORNIA
LAWRENCE LIVERMORE LABORATORY
P.O. BOX 808
LIVERMORE, CA 94550
  01CY ATTN DOC CON FOR TECH INFO DEPT
  01CY ATTN DOC CON FOR L-389 R. OTT
  01CY ATTN DOC CON FOR L-31 R. HAGER

LOS ALAMOS NATIONAL LABORATORY
P.O. BOX 1663
LOS ALAMOS, NM 87545
  01CY ATTN DOC CON FOR J. WOLCOTT
  01CY ATTN DOC CON FOR R.F. TASCHEK
  01CY ATTN DOC CON FOR E. JONES
  01CY ATTN DOC CON FOR J. MALIK
  01CY ATTN DOC CON FOR R. JEFFRIES
  01CY ATTN DOC CON FOR J. ZINN
  01CY ATTN DOC CON FOR D. WESTERVELT
  01CY ATTN D. SAPPENFIELD

SANDIA LABORATORIES
P.O. BOX 5800
ALBUQUERQUE, NM 87115
  01CY ATTN DOC CON FOR W. BROWN
  01CY ATTN DOC CON FOR A. THORNBROUGH
  01CY ATTN DOC CON FOR T. WRIGHT
  01CY ATTN DOC CON FOR D. DAHLGREN
  01CY ATTN DOC CON FOR 3141
  01CY ATTN DOC CON FOR SPACE PROJECT DIV

SANDIA LABORATORIES
LIVERMORE LABORATORY
P.O. BOX 969
LIVERMORE, CA 94550
  01CY ATTN DOC CON FOR B. MURPHEY
  01CY ATTN DOC CON FOR T. COOK

OFFICE OF MILITARY APPLICATION
DEPARTMENT OF ENERGY
WASHINGTON, D.C. 20545
  01CY ATTN DOC CON DR. YO SONG

OTHER GOVERNMENT

INSTITUTE FOR TELECOM SCIENCES
NATIONAL TELECOMMUNICATIONS & INFO
ADMIN
BOULDER, CO 80303
01CY ATTN A. JEAN (UNCLASS ONLY)
01CY ATTN W. UTLAUT
01CY ATTN D. CROMBIE
01CY ATTN L. BERRY

NATIONAL OCEANIC & ATMOSPHERIC ADMIN
ENVIRONMENTAL RESEARCH LABORATORIES
DEPARTMENT OF COMMERCE
BOULDER, CO 80302
01CY ATTN R. GRUBB
01CY ATTN AERONOMY LAB G. REID

DEPARTMENT OF DEFENSE CONTRACTORS

AEROSPACE CORPORATION
P.O. BOX 92957
LOS ANGELES, CA 90009
01CY ATTN I. GARFUNKEL
01CY ATTN T. SALMI
01CY ATTN V. JOSEPHSON
01CY ATTN S. BOWER
01CY ATTN D. OLSEN

ANALYTICAL SYSTEMS ENGINEERING CORP
5 OLD CONCORD ROAD
BURLINGTON, MA 01803
01CY ATTN RADIO SCIENCES

AUSTIN RESEARCH ASSOC., INC.
1901 RUTLAND DRIVE
AUSTIN, TX 78758
01CY ATTN L. SLOAN
01CY ATTN R. THOMPSON

BERKELEY RESEARCH ASSOCIATES, INC.
P.O. BOX 983
BERKELEY, CA 94701
01CY ATTN J. WORKMAN
01CY ATTN C. PRETTIE
01CY ATTN S. BRECHT

BOEING COMPANY, THE
P.O. BOX 3707
SEATTLE, WA 98124
01CY ATTN G. KEISTER
01CY ATTN D. MURRAY
01CY ATTN G. HALL
01CY ATTN J. KENNEY

CHARLES STARK DRAPER LABORATORY, INC.
555 TECHNOLOGY SQUARE
CAMBRIDGE, MA 02139
01CY ATTN D.B. COX
01CY ATTN J.P. GILMORE

COMSAT LABORATORIES
LINTHICUM ROAD
CLARKSBURG, MD 20734
01CY ATTN G. HYDE

CORNELL UNIVERSITY
DEPARTMENT OF ELECTRICAL ENGINEERING
ITHACA, NY 14850
01CY ATTN D.T. FARLEY, JR.

ELECTROSPACE SYSTEMS, INC.
BOX 1359
RICHARDSON, TX 75080
01CY ATTN H. LOGSTON
01CY ATTN SECURITY (PAUL PHILLIPS)

EOS TECHNOLOGIES, INC.
606 Wilshire Blvd.
Santa Monica, Calif 90401
01CY ATTN C.B. GABBARD
01CY ATTN R. LELEVIER

ESL, INC.
495 JAVA DRIVE
SUNNYVALE, CA 94086
01CY ATTN J. ROBERTS
01CY ATTN JAMES MARSHALL

GENERAL ELECTRIC COMPANY
SPACE DIVISION
VALLEY FORGE SPACE CENTER
GODDARD BLVD KING OF PRUSSIA
P.O. BOX 8555
PHILADELPHIA, PA 19101
01CY ATTN M.H. BORTNER
SPACE SCI LAB

GENERAL ELECTRIC TECH SERVICES
CO., INC.
HMES
COURT STREET
SYRACUSE, NY 13201
01CY ATTN G. MILLMAN

GEOPHYSICAL INSTITUTE
UNIVERSITY OF ALASKA
FAIRBANKS, AK 99701
(ALL CLASS ATTN: SECURITY OFFICER)
01CY ATTN T.N. DAVIS (UNCLASS ONLY)
01CY ATTN TECHNICAL LIBRARY
01CY ATTN NEAL BROWN (UNCLASS ONLY)

GTE SYLVANIA, INC.
ELECTRONICS SYSTEMS GRP-EASTERN DIV
77 A STREET
NEEDHAM, MA 02194
01CY ATTN DICK STEINHOF

HSS, INC.
2 ALFRED CIRCLE
BEDFORD, MA 01730
01CY ATTN DONALD HANSEN

ILLINOIS, UNIVERSITY OF
107 COBLE HALL
150 DAVENPORT HOUSE
CHAMPAIGN, IL 61820
(ALL CORRES ATTN DAN MCCLELLAND)
01CY ATTN K. YEH

INSTITUTE FOR DEFENSE ANALYSES
1801 NO. BEAUREGARD STREET
ALEXANDRIA, VA 22311
01CY ATTN J.M. AEIN
01CY ATTN ERNEST BAUER
01CY ATTN HANS WOLFARD
01CY ATTN JOEL BENGSTON

INTL TEL & TELEGRAPH CORPORATION
500 WASHINGTON AVENUE
NUTLEY, NJ 07110
01CY ATTN TECHNICAL LIBRARY

JAYCOR
11011 TORREYANA ROAD
P.O. BOX 85154
SAN DIEGO, CA 92138
01CY ATTN J.L. SPERLING

JOHNS HOPKINS UNIVERSITY
APPLIED PHYSICS LABORATORY
JOHNS HOPKINS ROAD
LAUREL, MD 20810
01CY ATTN DOCUMENT LIBRARIAN
01CY ATTN THOMAS POTEMRA
01CY ATTN JOHN DASSOULAS

KAMAN SCIENCES CORP
P.O. BOX 7463
COLORADO SPRINGS, CO 80933
01CY ATTN T. MEAGHER

KAMAN TEMPO-CENTER FOR ADVANCED
STUDIES
816 STATE STREET (P.O DRAWER QQ)
SANTA BARBARA, CA 93102
01CY ATTN DASIAC
01CY ATTN WARREN S. KNAPP
01CY ATTN WILLIAM MCNAMARA
01CY ATTN B. GAMBILL

LINKABIT CORP
10453 ROSELLE
SAN DIEGO, CA 92121
01CY ATTN IRWIN JACOBS

LOCKHEED MISSILES & SPACE CO., INC
P.O. BOX 504
SUNNYVALE, CA 94088
01CY ATTN DEPT 60-12
01CY ATTN D.R. CHURCHILL

LOCKHEED MISSILES & SPACE CO., INC.
3251 HANOVER STREET
PALO ALTO, CA 94304
01CY ATTN MARTIN WALT DEPT 52-12
01CY ATTN W.L. IMHOF DEPT 52-12
01CY ATTN RICHARD G. JOHNSON
DEPT 52-12
01CY ATTN J.B. CLADIS DEPT 52-12

MARTIN MARIETTA CORP
ORLANDO DIVISION
P.O. BOX 5837
ORLANDO, FL 32805
01CY ATTN R. HEFFNER

M.I.T. LINCOLN LABORATORY
P.O. BOX 73
LEXINGTON, MA 02173
  01CY ATTN DAVID M. TOWLE
  01CY ATTN L. LOUGHLIN
  01CY ATTN D. CLARK

MCDONNEL DOUGLAS CORPORATION
5301 BOLSA AVENUE
HUNTINGTON BEACH, CA 92647
  01CY ATTN N. HARRIS
  01CY ATTN J. MOULE
  01CY ATTN GEORGE MROZ
  01CY ATTN W. OLSON
  01CY ATTN R.W. HALPRIN
  01CY ATTN TECHNICAL
       LIBRARY SERVICES

MISSION RESEARCH CORPORATION
735 STATE STREET
SANTA BARBARA, CA 93101
  01CY ATTN P. FISCHER
  01CY ATTN W.F. CREVIER
  01CY ATTN STEVEN L. GUTSCHE
  01CY ATTN R. BOGUSCH
  01CY ATTN R. HENDRICK
  01CY ATTN RALPH KILB
  01CY ATTN DAVE SOWLE
  01CY ATTN F. FAJEN
  01CY ATTN M. SCHEIBE
  01CY ATTN CONRAD L. LONGMIRE
  01CY ATTN B. WHITE
  01CY ATTN R. STAGAT

MISSION RESEARCH CORP.
1720 RANDOLPH ROAD, S.E.
ALBUQUERQUE, NEW MEXICO 87106
  01CY R. STELLINGWERF
  01CY M. ALME
  01CY L. WRIGHT

MITRE CORP
WESTGATE RESEARCH PARK
1820 DOLLY MADISON BLVD
MCLEAN, VA 22101
  01CY ATTN W. HALL
  01CY ATTN W. FOSTER

PACIFIC-SIERRA RESEARCH CORP
12340 SANTA MONICA BLVD.
LOS ANGELES, CA 90025
  01CY ATTN E.C. FIELD, JR.

PENNSYLVANIA STATE UNIVERSITY
IONOSPHERE RESEARCH LAB
318 ELECTRICAL ENGINEERING EAST
UNIVERSITY PARK, PA 16802
  (NO CLASS TO THIS ADDRESS)
  01CY ATTN IONOSPHERIC RESEARCH LAB

PHOTOMETRICS, INC.
4 ARROW DRIVE
WOBURN, MA 01801
  01CY ATTN IRVING L. KOFSKY

PHYSICAL DYNAMICS, INC.
P.O. BOX 3027
BELLEVUE, WA 98009
  01CY ATTN E.J. FREMOUW

PHYSICAL DYNAMICS, INC.
P.O. BOX 10367
OAKLAND, CA 94610
  ATTN A. THOMSON

R & D ASSOCIATES
P.O. BOX 9695
MARINA DEL REY, CA 90291
  01CY ATTN FORREST GILMORE
  01CY ATTN WILLIAM B. WRIGHT, JR.
  01CY ATTN WILLIAM J. KARZAS
  01CY ATTN H. ORY
  01CY ATTN C. MACDONALD

RAND CORPORATION, THE
1700 MAIN STREET
SANTA MONICA, CA 90406
  01CY ATTN CULLEN CRAIN
  01CY ATTN ED BEDROZIAN

RAYTHEON CO.
528 BOSTON POST ROAD
SUDBURY, MA 01776
  01CY ATTN BARBARA ADAMS

RIVERSIDE RESEARCH INSTITUTE
330 WEST 42nd STREET
NEW YORK, NY 10036
  01CY ATTN VINCE TRAPANI

SCIENCE APPLICATIONS, INC.
1150 PROSPECT PLAZA
LA JOLLA, CA 92037
01CY ATTN LEWIS M. LINSON
01CY ATTN DANIEL A. HAMLIN
01CY ATTN E. FRIEMAN
01CY ATTN E.A. STRAKER
01CY ATTN CURTIS A. SMITH

SCIENCE APPLICATIONS, INC
1710 GOODRIDGE DR.
MCLEAN, VA 22102
01CY J. COCKAYNE
01CY E. HYMAN

SRI INTERNATIONAL
333 RAVENSWOOD AVENUE
MENLO PARK, CA 94025
01CY ATTN J. CASPER
01CY ATTN DONALD NEILSON
01CY ATTN ALAN BURNS
01CY ATTN G. SMITH
01CY ATTN R. TSUNODA
01CY ATTN DAVID A. JOHNSON
01CY ATTN WALTER G. CHESNUT
01CY ATTN CHARLES L. RINO
01CY ATTN WALTER JAYE
01CY ATTN J. VICKREY
01CY ATTN RAY L. LEADABRAND
01CY ATTN G. CARPENTER
01CY ATTN G. PRICE
01CY ATTN R. LIVINGSTON
01CY ATTN V. GONZALES
01CY ATTN D. MCDANIEL

TECHNOLOGY INTERNATIONAL CORP
75 WIGGINS AVENUE
BEDFORD, MA 01730
01CY ATTN W.P. BOQUIST

TOYON RESEARCH CO.
P.O. Box 6890
SANTA BARBARA, CA 93111
01CY ATTN JOHN ISE, JR.
01CY ATTN JOEL GARBARINO

TRW DEFENSE & SPACE SYS GROUP
ONE SPACE PARK
REDONDO BEACH, CA 90278
01CY ATTN R. K. PLEBUCH
01CY ATTN S. ALTSCHULER
01CY ATTN D. DEE
01CY ATTN D/ STOCKWELL
SNTF/1575

VISIDYNE
SOUTH BEDFORD STREET
BURLINGTON, MASS 01803
01CY ATTN W. REIDY
01CY ATTN J. CARPENTER
01CY ATTN C. HUMPHREY

UNIVERSITY OF PITTSBURGH
PITTSBURGH, PA 15213
01CY ATTN: N. ZABUSKY

DIRECTOR OF RESEARCH
U.S. NAVAL ACADEMY
ANNAPOLIS, MD 21402
02CY

END

FILMED

1-86

DTIC